ANL/ET/CP-97443

TRIBOLOGICAL PROPERTIES OF NANOCRYSTALLINE DIAMOND FILMS*

A. Erdemir, G. R. Fenske, A. R. Krauss, D. M. Gruen , T. McCauley, and R. T. Csencsits
Energy Technology, Materials Science, and Chemistry Divisions
Argonne National Laboratory
Argonne, IL 60439

Revised, May 1999

Invited paper presented at the 1999 International Conference on Metallurgical Coatings and Thin Films, San Diego, CA, April 12-16, 1999

*Work supported by the U.S. Department of Energy under Contract W-31-109-Eng-38.

DISCLAIMER

TRIBOLOGICAL PROPERTIES OF NANOCRYSTALLINE DIAMOND FILMS

A. Erdemir, G. R. Fenske, A. R. Krauss, D. M. Gruen, T. McCauley, and R. T. Csencsits
Energy Technology, Materials Science, and Chemistry Divisions
Argonne National Laboratory
Argonne, IL 60439

ABSTRACT

In this paper, we present the friction and wear properties of nanocrystalline diamond (NCD) films grown in Ar-fullerene (C_{60}) and Ar-CH_4 microwave plasmas. Specifically, we will address the fundamental tribological issues posed by these films during sliding against Si_3N_4 counterfaces in ambient air and inert gases. Grain sizes of thefilms grown by the new method are very small (10-30 nm) and are much smoother (20-40 nm, root mean square) than those of films grown by the conventional H_2-CH_4 microwave-assisted chemical-vapor-deposition (CVD) process. Transmission electron microscopy (TEM) revealed that the grain boundaries of these films are very sharp and free of nondiamond phases. The microcrystalline diamond (MCD) films grown by most conventional methods consist of large grains and a rough surface finish, which can cause severe abrasion during sliding against other materials. The friction coefficients of films grown by the new method (i.e., in Ar-C_{60} and Ar- CH_4 plasmas) are comparable to those of natural diamond, and wear damage on counterface materials is minimal. Fundamental tribological studies indicate that these films may undergo phase transformation during long-duration, high-speed and/or high-load sliding tests and that the transformation products trapped at the sliding interfaces can intermittently dominate friction and wear performance. Using results from a combination of TEM, electron diffraction, Raman spectroscopy, and electron energy loss spectroscopy (EELS), we describe the structural chemistry of the debris particles trapped at the sliding interfaces and elucidate their possible effects on friction and wear of NCD films in dry N_2. Finally, we suggest a few potential applications in which NCD films can improve performance and service lives.

INTRODUCTION

Recently, interest in producing high-quality, smooth diamond films on metallic and ceramic substrates for use in a various engineering applications has been overwhelming . The reson for the interest is that the properties of diamond i.e., the highest hardness, stiffness, and thermal conductivity as well as imperviousness to acidic and saline media, are exceptional and far exceed those of any other known material. Moreover, cleaved diamond surfaces exhibit one of the lowest friction coefficients of any known material. The combination of these qualities in a material is ideal for highly demanding tribological applications. In fact, if it were inexpensive and abundant, diamond would undoubtedly be the material of choice for many tribological applications.

Prospects for large-scale uses of diamond in tribology increased sharply when researchers discovered that diamond can be grown as thin films at low deposition pressures (10^2-10^3 Pa) from hydrocarbon/hydrogen mixtures by chemical vapor deposition (CVD) methods, including plasma-enhanced CVD, hot-filament CVD, microwave CVD, DC-arc jets, etc. [1-4]. Plasma conditions in these methods are tailored to dissociate hydrocarbon/hydrogen mixtures into ionic or highly energetic species that are essential for the initial nucleation as well as subsequent growth of these films. Diamond can be deposited on certain metallic and ceramic substrates with excellent bonding. Typical substrate temperatures for diamond deposition are 600-950°C. Deposition of diamond at temperatures below 600°C has also been demonstrated but growth rates are drastically reduced and the amount of nondiamond precursors in these films is substantially greater.

High-quality microcrystalline diamond (MCD) films exhibit most of the desired properties of natural diamonds. They are made up of large columnar grains that are highly faceted and generally rough.

They tend to grow continuously rougher as the thickness of the deposited films increases. The generally rough surface finish of these films precludes their immediate uses for most machining and wear applications. When used in sliding-wear applications, such rough films cause high friction and very high wear losses on mating surfaces [5-7]. The rough MCD films can be polished by laser beams, fine diamond powders, or by rubbing against a hot iron plate [8]. Figure 1 shows the surface morphology of a PCD film before and after laser polishing. Friction coefficients of the polished films can be comparable to the friction coefficient of natural diamond [9,10]. However, the polishing processes are tedious, take very long time, and, in the case of complex geometries, they are very impractical. Despite high interest in using diamond films for diverse tribological applications, their widespread utilization in the industrial world has not yet met expectations [11-15]. Until now, only certain cemented carbide (i.e., WC-Co) and ceramic tools (i.e., Si_3N_4) have been coated successfully with diamond and made available commercially. Although prototypes of other tribological parts (such as mechanical seals) have been prepared with diamond films, their large-scale utilization has not yet been realized.

Recently, new methods have been developed for the deposition of smooth, nanocrystalline diamond (NCD) films using a higher-than-normal C/H ratio in a microwave plasma or by applying a DC bias to the substrates [16]. Although growth rates were somewhat reduced, the surface finish of the resulting diamond films was much smoother (i.e., 25 nm, RMS) and their friction coefficients were 0.05-0.1, depending on the test environment. Deposition of NCD films has also been achieved by using Ar-C_{60} and Ar-CH_4 plasmas in a modified microwave CVD system [17]. The grains of the films were very small (i.e., 10-30 nm) and their surface finish was 20-40 nm, RMS.

The primary goal of this paper is to provide an overview of recent developments in the production and tribology of NCD films. A brief description of the friction and wear mechanisms of these films under dry sliding conditions will be presented first. We will then discuss the fundamental issues associated with film microstructure and chemistry. In terms of structural and fundamental tribological knowledge, the paper will describe deposition conditions that lead to the formation of an ideal film that affords ultralow friction and wear in sliding tribological applications.

DEPOSITION OF NCD FILMS

The deposition of NCD films at Argonne National Laboratory (ANL) is achieved in a microwave plasma that consists primarily of Ar, with either C_{60}, or CH_4 as the carbon precursor in the near absence of atomic hydrogen. The reactor used for the process is essentially a modified ASTeX system (Model: PDS-17), details of which can be found in Refs. 17 and 18. A schematic illustration of this system is depicted in Fig. 2. To introduce C_{60} into the reactor, a quartz transpirator (shown in Fig. 2) was attached. Fullerene-rich soots, consisting of approximately 10% C_{60}, were placed in the transpirator. The soot was heated to 200°C under vacuum for 2 h to remove residual gases and hydrocarbons. During operation, the tube furnace and transport tube were heated to between 550 and 600°C to sublime C_{60} into the gas phase. Argon gas was passed through the transpirator to carry the C_{60} vapor into the plasma. To ensure that C_{60} was transported into the chamber, a silicon wafer was placed in front of the transport tube while maintaining a 14 sccm argon flow. With the reactor pressure at 100 torr and the transpirator at 600°C, a 1.7-mg brown film was deposited on the wafer in 1 h. The film displayed only strong C_{60} infrared absorption features. The measured Raman spectrum was also attributed to C_{60}. On the basis of these measurements, the transpirator is considered an effective source of C_{60} for diamond growth. The NCD films can also be grown under similar low hydrogen content conditions with CH_4 instead of C_{60} as the carbon source.

The NCD films can be grown on a variety of substrates, including single-crystal silicon wafers, sintered SiC, W, WC, Si_3N_4, etc. Initially, a bias of -150 V is applied to enhance the density of diamond nucleation. Film growth is monitored insitu by laser reflectance interferometry to determine growth rate and to stop growth at the desired film thickness. The substrate temperature may vary between 700 and 950°C, and the total gas flow rate is around 100 sccm. A typical gas composition for NCD diamond film can be 97% Ar, 2% H_2 and 1% C_{60} or CH_4 at a total pressure of 1.33×10^4 Pa and a microwave power of 800 W. Figure 3 shows cross-sectional and plan-view SEM and TEM photomicrographs of an NCD film produced at ANL.

The growth mechanism of NCD films differs significantly from that of conventional diamond films produced by other CVD methods, as addressed in a series of recent papers [19-21]. Specifically, a carbon dimer extraction from C_{60} and CH_4 molecules and subsequent insertion has recently been proposed for the growth of these films. C_2 dimers are the major diamond growth species and are inserted directly to the diamond surface. In the case of conventional diamond growth processes, small diamond grains are rapidly etched by atomic hydrogen and growth of larger grains is kinetically preferred over formation of new diamond nuclei. The low levels of atomic hydrogen inANL's process permit continuous renucleation of the diamond phase, and promote formation of films with a very small grain [22]. The resultant films are phase-pure NCD, with an average grain size of ~15 nm as can be seen in the plan-view and cross-sectional TEM photomicrographs in Figs. 3 b and c. The C_2 dimer growth mechanism is unique in that it is capable of producing a continuous diamond coating that can be as thin as 30-60 nm.

Figure 4 shows UV Raman spectra of high-quality C_{60}-grown NCD and CH_4-grown MCD films. As is known, UV-excited Raman spectroscopy is most sensitive to sp^3-bonded carbon [23]. In both

cases, the Raman bands at ≈1332 cm^{-1} are rather sharp and attributed to diamond. The spectrum of the NCD film contains an additional broad feature at 1580 cm^{-1} that is attributed to sp^2 carbon which is present at the boundaries between many grains in these films. The amount of sp^2-bonded carbon at the grain boundaries of NCD films was estimated to be ≈ 1 to 2 at.% [24].

TRIBOLOGY OF NCD FILMS

As elaborated above, conventional MCD films are generally rough and consist of large grains (see Fig. 1). Depending on deposition conditions, these grains exhibit <111> or <100> crystallographic growth orientations. Figure 5 shows the friction coefficients of MCD (surface roughness: 0.35 μm, rms) and NCD (surface roughness: 30 nm, rms) films against Si_3N_4 balls in open air and dry N_2. After an initial run-in period during which friction is relatively high, the friction coefficient of the NCD film decreases rapidly to ≈ 0.1 in open air and to 0. ≈ 05 in dry N_2, whereas the friction coefficient of the MCD film remains high and unsteady in both test environments.

Wear rates of Si_3N_4 balls slid against the smooth NCD and rough MCD films in air and dry N_2 are shown in Fig. 6 which clearly shows that the wear rates of balls slid against the NCD films are more than 2 orders of magnitude lower than the wear rates of balls slid against the rough MCD films. The high friction coefficients of rough diamond films can be attributed to the abrasive cutting and plowing effects of sharp asperity tips on softer counterface pins, whereas the plowing effects created by smooth NCD films on counterface balls are minimal and thus exhibit lower friction. Previous studies also demonstrated a close correlation between higher surface roughness and greater frictional losses [6,9,10,25,26]. As mentioned earlier, the rough MCD films can be polished, and when such polished films are used in sliding-contact experiments, very low friction coefficients are obtained [9,10,16,25-29].

Apart from physical roughness, surface chemistry and tribo-induced adhesive interactions can also occur and play a dominant role in the friction and wear performance of all diamond films [30]. The nature and extent of interactions may be controlled by the environmental species or by ambient temperature [31]. Mechanistically, the low-friction nature of smooth or cleaved diamond surfaces has long been attributed to the highly passive nature of their surfaces [32-35]. Specifically, it has been postulated that gaseous adsorbates, such as hydrogen, oxygen, or water vapor, can effectively passivate the dangling surface bonds of diamond. When the dangling bonds become highly passive, the adhesion component of friction is diminished. Recent fundamental studies by Gardos and his coworkers have shown that, when adsorbed gases are thermally desorbed from the sliding diamond surfaces, the friction coefficient increases rapidly. Because the dangling surface bonds of diamond are reactivated and hence available to form strong adhesive bonds across the sliding contact interfaces [36-39]. Furthermore, they also showed that the reconstructed diamond surfaces (which can occur at high-temperatures) exhibit reduced-friction. In short, previous research has shown that the lowest adhesion or friction on sliding diamond surfaces is achieved when dangling bonds are fully passivated by gaseous adsorbates (preferably hydrogen) [30-40].

Phase transformations due to extreme contact pressures and high frictional heating at local asperities can also occur and dominate the friction and wear behavior of diamond films. Most often, contact occurs first between sharp asperity tips, which can either fracture or undergo phase transformation because of high mechanical and thermal loadings. The logic behind such a transformation is that under such extreme conditions, the real contact spots of a diamond may be activated or forced to undergo phase transformation or graphitization [41]. Thermodynamically, graphite is the most stable form of carbon, whereas diamond is unstable. Graphite debris particles can gradually accumulate at the sliding

contact interface and then begin to dominate the long-term friction and wear performance of diamond films.

Figure 7 shows the variation of the friction coefficients of a Si_3N_4 ball slid against an NCD film (surface roughness:35 nm, RMS) during relatively long-duration tests (22,000 cycles) in dry N_2. It is clear from the figure that the initial friction coefficient is high (0.6), decreases rapidly as sliding continues, and stabilizes at 0.06. Note that the friction occasionally increases to values as high as 0.55 but decreases back to the 0.06 level. The friction coefficient of the same test pair in air was 0.12 and did not fluctuate much throughout the long-duration test. This disparity between friction coefficient of NCD films in air (0.12) and dry N_2 (0.06) is explained below.

Under the combined influence of highly concentrated normal and shear forces and frictional heating during sliding, the moving asperity tips of diamond films may undergo gradual phase transformation and hence micromechanical wear. It is possible that asperity tips of diamond may first be chipped away without phase transformation, become trapped at the sliding interface, and then undergo further wear and phase transformation under the influence of repeated sliding passes [42]. Diamond, which is thermodynamically unstable, can be transformed to a more stable carbon form, such as graphite when excited thermally or by ion bombardment [43,44].

As phase transformation continues and the graphitic debris particles accumulate at the sliding interface, they can intermittently cause high friction coefficients in dry N_2, as shown in Fig. 7. Conversely, as the debris layer wears out or is removed from the sliding interface by mechanical means, low friction once again prevails. This low-friction regime persists for a time and, as the graphitic debris gradually builds up again at the sliding interface and reaches a critical level, the

friction coefficient increases to 0.5. Graphite is a poor lubricant in vacuum or dry test environments. Briefly, we believe that the physical and/or tribochemical changes that occur at sliding interfaces are the major reason for the steep transitions in the frictional behavior of diamond films in dry N_2.

To further elucidate the mechanistic explanation given above, the structural chemistry of the debris particles as well as the sliding contact surfaces were investigated by laser Raman spectroscopy, electron energy loss spectroscopy (EELS), electron diffraction, and TEM to provide complementary and more convincing information on the phase transformation of sliding diamond surfaces [42]. The results of Raman studies showed that the wear debris particles that are formed in dry N_2 and accumulate in and around the wear scars and tracks, as well as the wear debris particles of a smeared transfer layer on the ball wear scar are quite similar to graphite but are different from the wear debris particles of the as-deposited diamond film (Fig. 8). Specifically, two broad Raman features of the loose debris particles and transfer layers centered at 1330 and 1580 cm^{-1} match the D and G band energies of crystalline graphite. This finding suggests that debris particles present at the sliding interface are in a graphitic state.

Further examination of debris particles by electron diffraction, EELS, and TEM confirmed the formation of a highly disordered graphitic structure, as shown in Fig. 9. Specifically, the energy-loss features of the carbon K edge in the EELS spectrum and the shape of this edge provided information about the nature of the bulk carbonaceous precursor. In particular, a feature known as π^* (at 285 eV) is present only for the sp^2-bonded form of carbon and is absent for the sp^3-bonded carbon atoms, as in crystalline diamond. The K edge of debris particles presented a shouldered π^* feature at 285 eV, suggesting that it consisted of an sp^2-bonded carbon form, whereas the electron diffraction pattern revealed a pseudoamorphous state for the same debris particles; the TEM image presented in Fig.

9a. Thus, from these analytical findings, one can conclude that the carbonaceous precursor in the debris particles was made up mainly of sp^2-bonded carbon.

Briefly, based on the combination of surface and structure analytical results (i.e., Raman, TEM, and EELS), we propose that during sliding in dry N_2, diamond films can be transformed to a disordered graphitic state. Friction spikes seen during tests in dry N_2 are typical of the high-friction nature of graphite in dry environments.

SUMMARY AND FUTURE DIRECTION

Diamond films have much to offer for future tribological applications. Unlike most other engineering materials, diamond offers a combination of low friction and high wear resistance under a wide range of sliding-contact conditions. The roughness of PCD films limited their use in commercial applications. Over the years, great strides have been made in overcoming problems associated with surface roughness. Currently, methods are available to deposit smooth diamond films on a various substrates. A variety of effective methods are also available for polishing rough PCD films. Smooth diamond films can be used in mechanical-seal applications, and for protection against wear and as abrasion resistant coatings in several demanding tribological applications.

The results of tribological studies suggest that depending on the tribological and environmental constraints, adsorption and desorption of gaseous species, surface reconstruction at high temperatures, and graphitization in inert test environments can occur at sliding contact interfaces of diamond films and control their friction and wear behavior.

Smooth diamond films described in this study exhibited low friction and wear against sliding Si_3N_4

counterfaces. Friction coefficients in open air were ≈0.1, but fluctuated substantially in dry N_2 (i.e., varied between 0.06 and 0.55), especially during long-duration tests. Combined results from Raman, electron diffraction, EELS, and TEM studies led us to conclude that the structure of wear debris particles generated at sliding interfaces in dry N_2 is that of a disordered graphite. Graphite is not a good lubricant in dry environments; hence is responsible for large fluctuations in the friction of NCD films in dry N_2.

ACKNOWLEDGMENTS

This work is supported by the U.S. Department of Energy, under Contract W-31-109-Eng-38.

REFERENCES

1. J. Angus, in Synthetic Diamond: Emerging CVD Science and Technology, eds. K. E. Spear and J. P. Dismukes (John Wiley & Sons, Inc., New York, 1994), p. 21.

2. "Status and Applications of Diamond and Diamond-like Materials: An Emerging Technology," National Materials Advisory Board, Washington, DC, (1990)

3. W. J. P. van Enckevort, J. Hard Mater., 1 (1990) 247.

4. S. J. Bull, Diamond Rel. Mater., 4 (1995) 827.

5. D. G. Bhat, D. G. Johnson, A. P. Malshe, H. Naseem, W. D. Brown, L. W. Schaper, and C.-H. Shen, Diamond and Related Mat., 4 (1995) 921.

6. I. P. Hayward, Surf. Coat. Technol., 49 (1991) 554.

7. A. K. Gangopadhyay and M. A. Tamor, Wear, Wear, 169 (1993)221.

8. S. K. Choi, D. Y. Jung, S. Y. Kweon and S. K. Jung, Thin Solid Films, 279 (1996) 110.

9. A. Erdemir, M. Halter, G. R. Fenske, A. Krauss, D. M. Gruen, S. M. Pimenov, V. I. Konov, Surf. Coat. Technol., 94-96 (1997) 537.

10. B. Buhshan, V. V. Subramanian, A. Malshe, B. K. Gupta, and J. Ruan, J. Appl. Phys., 74 (1993) 41.

11. B. E. Williams and J. T. Glass, J. Mater. Res., 4 (1989) 373.

12. S. Chikata, MRS Bull., 23 (9) (1998)61

13. M. Seal, Applications of Diamond Films and Related Materials: 3rd Int. Conf., eds., A. Feldman et al., NIST Special Publication 885, pp. 3-12 (1995).

14. S. J. Bull and A. Mathews, Diamond and Rel. Mat., 1 (1992) 1049.

15. K.V. Ravi, Synthetic Diamond: Emerging CVD Science and Technology, eds., K. E. Spear, and J. P. Dismukes, ISBN 0-471-53589-3, Electrochem. Soc. Monograph (John Wiley and Sons, New York, 1994), pp. 419-504.

16. S. Hogmark, O. Hollman, A. Alahelisten, and P. Hedenqvist, Wear, 200 (1996) 235.

17. D.M. Gruen, S. Liu, A.R. Krauss, and X. Pan, J. Appl. Phys., 75 (1994)1758.

18. D.M. Gruen, S. Liu, A.R. Krauss, J. Luo, and X. Pan, Appl. Phys. Lett. 64 (1994)1502.

19. D. A. Horner, L. A. Curtiss, and D. M. Gruen, Chem. Phys. Lett., 233 (1995) 234.

20. P. C. Redfern, D. A. Horner, L. A. Curtiss, and D. M. Gruen, J. Phys. Chem., 100 (1996) 11654.

21.D. M. Gruen, C. D. Zuiker, A. R. Krauss, and X. Pan, J. Vac. Sci. Technol. A 13(3), (1995) 1628.

22. D. M. Gruen, MRS Bull., 23 (9) (1998) 32.

23. R. W. Bormett, S. A. Asher, R. E. Witkowski, W. D. Partlow, R. Lizewski, and F. Petit, J. Appl. Phys., 77(1995) 5916.

24. D. M. Gruen, A. R. Krauss, C. D. Zuiker, R. Csencsits, L. J. Terminello, J. A. Carlisle, I. Jimenes, D. G. Sutherlan, D. K. Shuh, W. Tong, and F. J. Himpsel: Appl. Phys. Let. 68 (1996) 1640.

25. I. P. Hayward, I. L. Singer, and L. E. Seitzman, Wear, 157 (1992) 215.

26. K. Miyoshi, R. L. C. Wu, A. Arscadden, N. Barnes, and L. Jackson, J. Appl. Phys., 74 (1993) 4446.

27. C. Zuiker, A. R. Krauss, D. M. Gruen, X. Pan, J. C. Li, R. Csencsits, A. Erdemir, C. Bindal, and G. Fenske, Thin Solid Films 270 (1995) 154.

28. A. Erdemir, G. R. Fenske, and C. Bindal, C. Zuiker, A. Krauss, D. Gruen, Diamond Rel. Mater., 5 (1996) 923.

29. A. Erdemir, C. Bindal, G. R. Fenske, C. Zuiker, R. Csencsits, A. R. Krauss, and D. M. Gruen, Diamond Films Technol., 5 (1996) 923.

30. M. N. Gardos and K. V. Ravi, Diamond Films Technol., 4 (1994) 139.

31. M. N. Gardos and B. L. Soriano, J. Mater. Res., 5 (1990) 2599.

32. F. P. Bowden and J. E. Young: Proc. Royal Soc. London, 208 (1951) 444.

33. F. P. Bowden and A. E. Hanwell: Proc. Royal Soc. London, A295 (1966) 233.

34. S. V. Pepper, J. Vac. Sci. Technol., 20 (1982) 643.

35. S. Chandrasekar and B. Bhushan, Wear, 153 (1992) 79.

36. M. N. Gardos, Trib. Lett., 2(1996)173.

37. M.N. Gardos, Tribol. Lett., 2 (1996) 355.

38. M. N. Gardos, Trib. Lett., 4^{s}(1998)175

39. M.N. Gardos, Protective Coatings and Thin Films, Proc. NATO Adv. Res. Workshop, May 29 - June 5, 1996, NATO ARW Series, eds., Y. Pauleau and P.B. Barna (Kluwer Academic Publishers, Dordrecht, The Netherlands, 1997), p.185.

40. M. Dugger, D. E. Peebles, and L. E. Pope, Surface Science Investigations in Tribology, Experimental Approaches, eds., Y.-W. Chung, A. M. Homolo, and G. B. Street, ACS Symp. Series 485, (American Chemical Society, Washington, DC, 1992), pp. 72-102.

41. A. Erdemir, C. Bindal, G. R. Fenske, and P. Wilbur, Tribol. Trans., 39 (1996) 735.

42. A. Erdemir, M. Halter, G. R. Fenske, R. Csencsits, A. R. Krauss, and D. M. Gruen, Tribol. Trans., 40 (1997) 667.

43. E. H. Lee, D. M. Hembree, G. R. Rao, and L. K. Mansur, Phys. Rev., 48 (1993) 15540.

44. E. H. Lee, M. B. Lewis, P. J. Blau, and L. K. Mansur, J. Mater. Res., 6 (1991) 610.

FIGURE CAPTION:

Figure 1. Surface morphology of a PCD film (a) before and (b) after laser polishing.

Figure 2. A schematic illustration of the modified microwave CVD system used in the deposition of Argonne's NCD films.

Figure 3. Cross-sectional and plan-view SEM and TEM photomicrographs of NCD films.

Figure 4. UV-Raman spectrum of C_{60}-grown NCD and CH_4-PCD films.

Figure 5. Friction coefficients of rough PCD and smooth NCD films against Si_3N_4 balls in (a) open air and (b) in dry N_2 (Test Conditions: Load, 2 N; Velocity, 0.05 m/s; Relative Humidity, 37%; Sliding Distance, 40 m; Ball Diameter, 9.55 mm)

Figure 6. Wear rates of Si_3N_4 balls slid against smooth NCD and rough PCD films in air and dry N_2 (Test Conditions: Load, 2 N; Velocity, 0.05 m/s; Relative Humidity, 37%; Sliding Distance, 40 m; Ball Diameter, 9.55 mm).

Figure 7. Variation of the friction coefficient of Si_3N_4 ball against NCD film (surface roughness: 35 nm, RMS) during a relatively long duration test (22,000 cycles, 6 hours) in dry N_2 (Test Conditions: Load, 2 N; Velocity, 0.06 m/s; Relative Humidity, 0%; Sliding Distance, 410 m; Ball Diameter, 9.55 mm).

Figure 8. Raman spectra of wear debris particles and transfer layers formed on Si_3N_4 ball during sliding in dry N_2.

Figure 9. (a) TEM photomicrograph and electron diffraction and (b) EELS of debris particles collected from sliding surfaces of NCD films and Si_3N_4 balls.

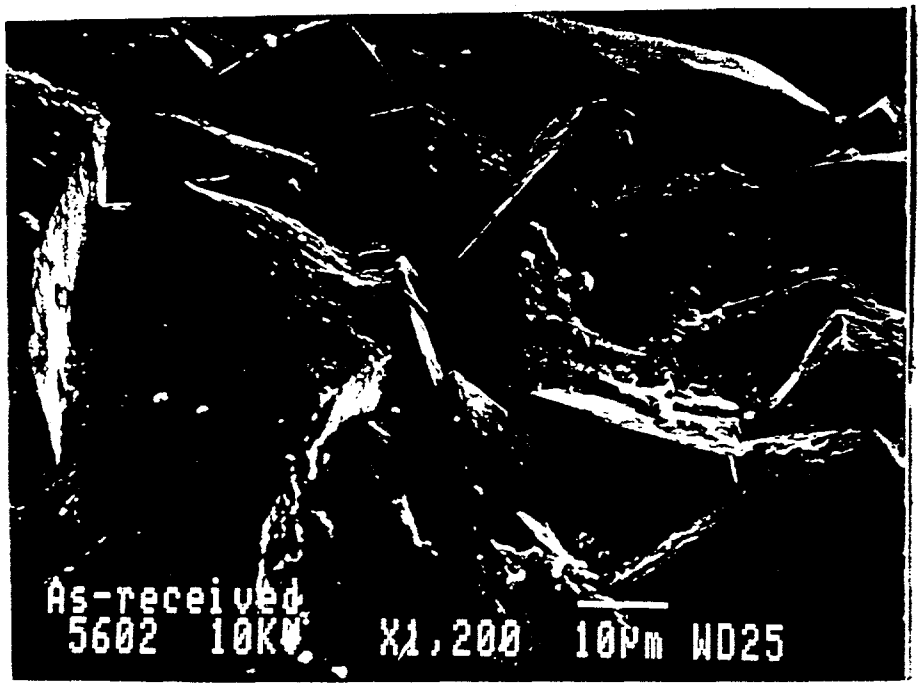
As-received
5602 10KV X1,200 10Pm WD25

(a)

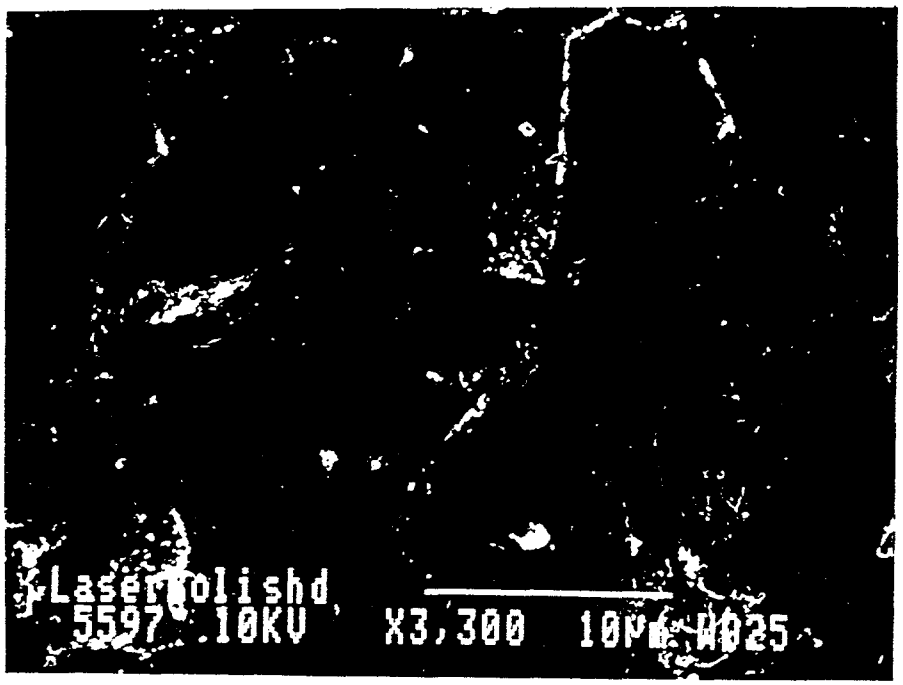
Laser polishd
5597 10KV X3,300 10Pm WD25

(b)

Figure 1.

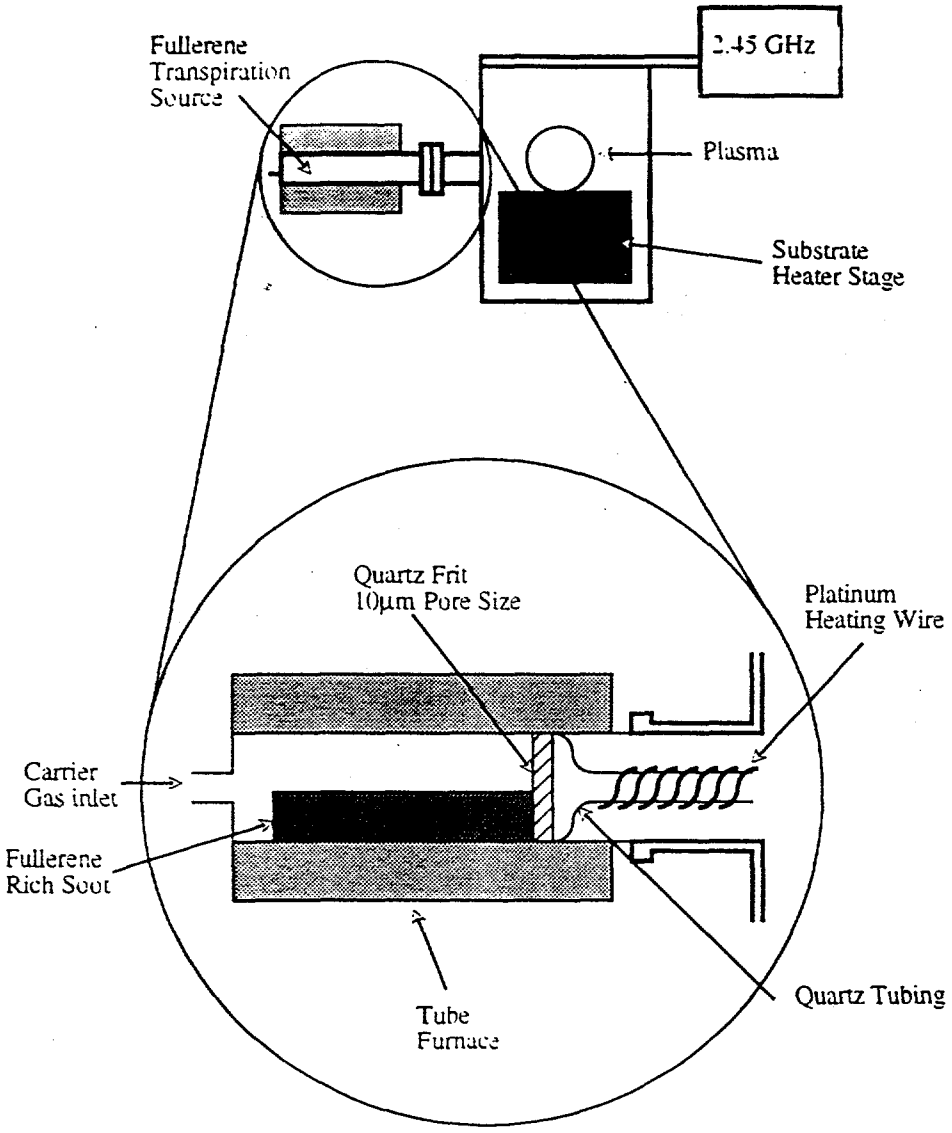
Fullerene
Transpiration
Source
2.45 GHz
Plasma
Substrate
Heater Stage
Quartz Frit
10μm Pore Size
Platinum
Heating Wire
Carrier
Gas inlet
Fullerene
Rich Soot
Tube
Furnace
Quartz Tubing

Figure 2.

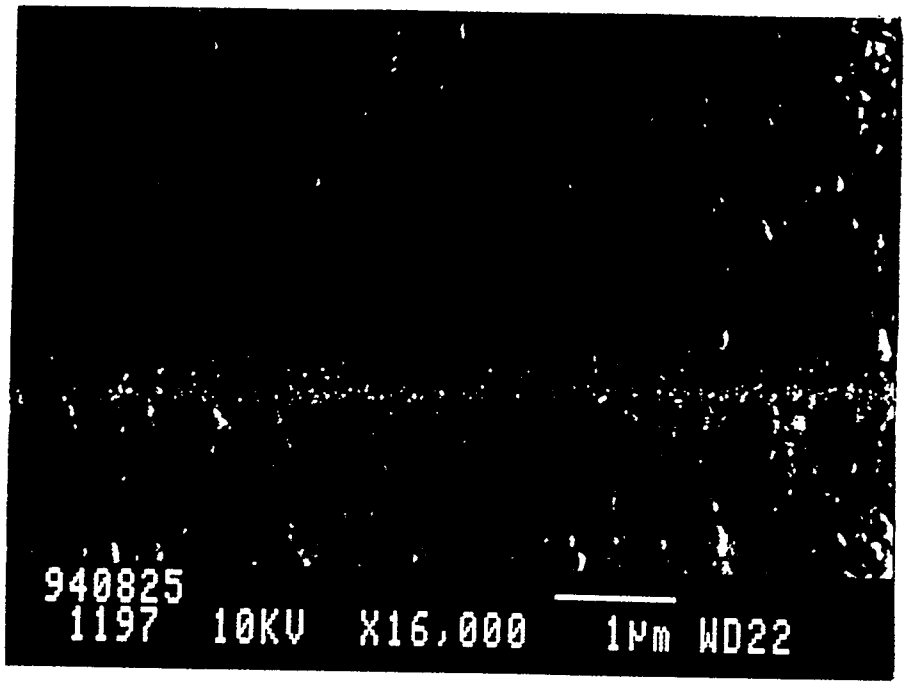

(a) Plan-view SEM

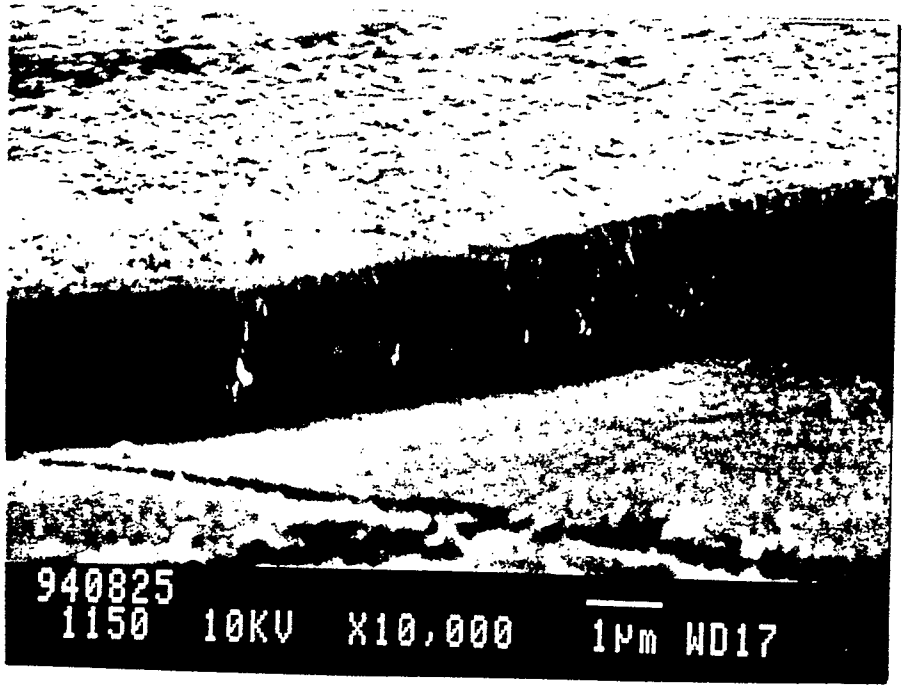

(b) Cross-sectional SEM

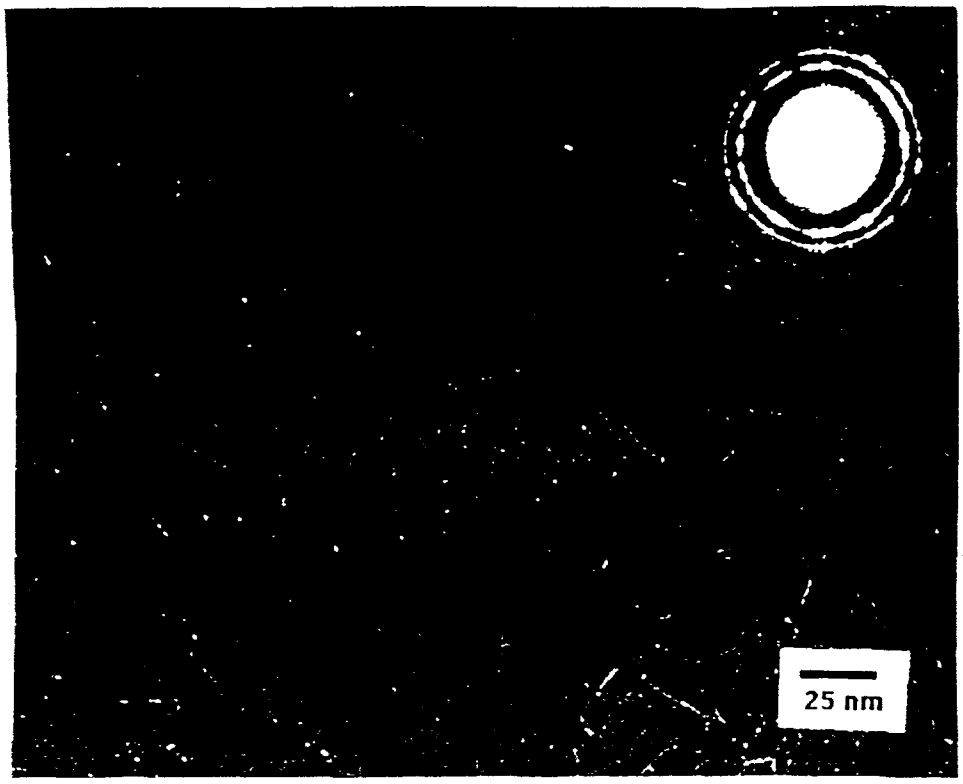

(c) Plan-view TEM

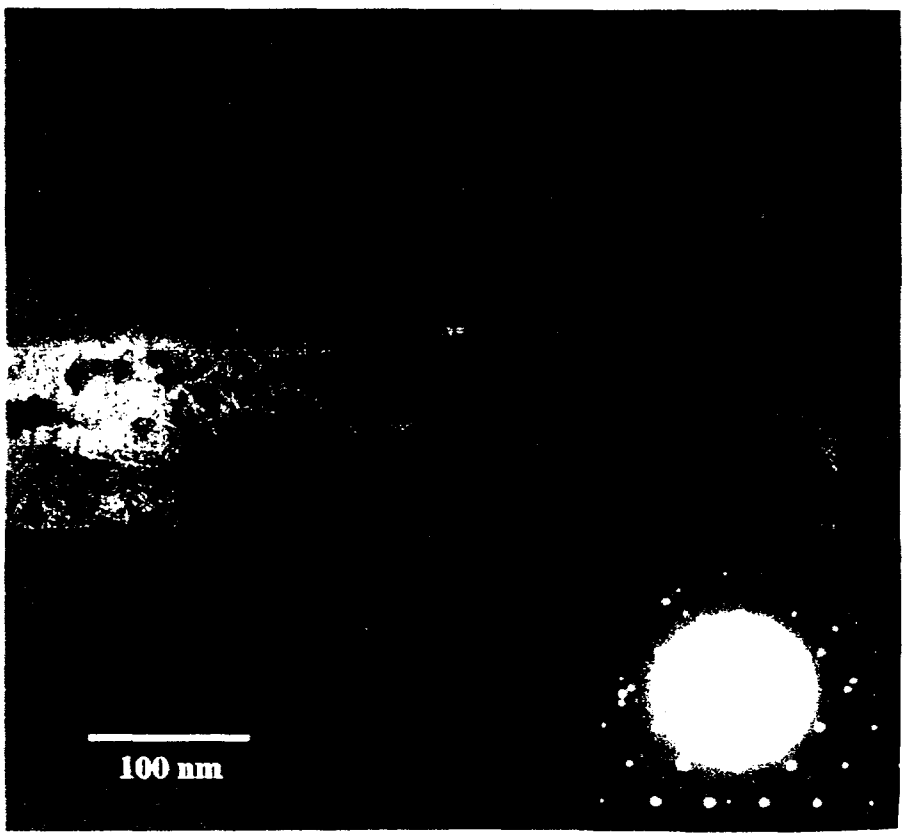

(d) Cross-sectional TEM

Figure 3

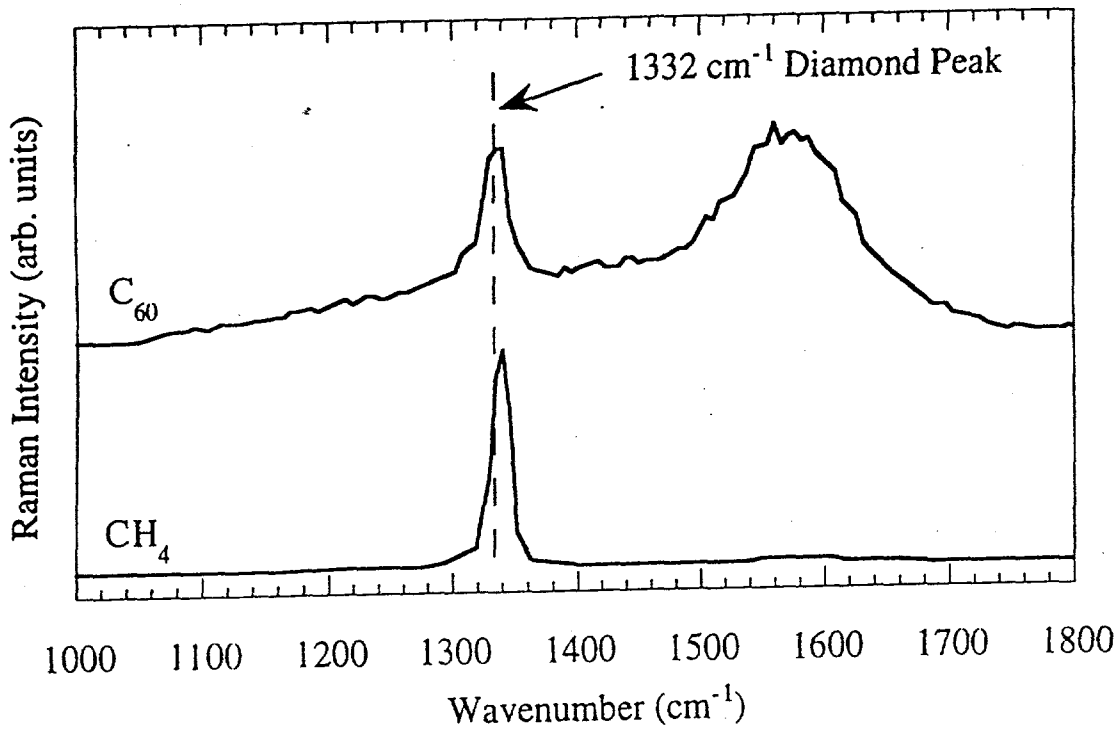
1332 cm-1 Diamond Peak
C60
CH4
Raman Intensity (arb. units)
1000
1100
1200
1300
1400
1500
1600
1700
1800
Wavenumber (cm-1)

Figure 4.

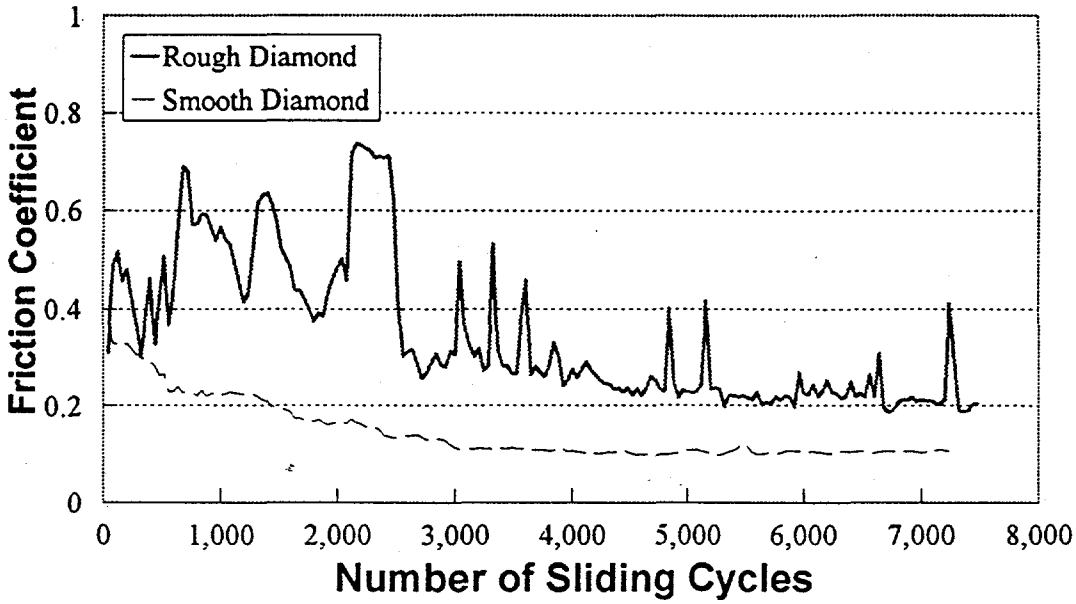

Figure 5a.

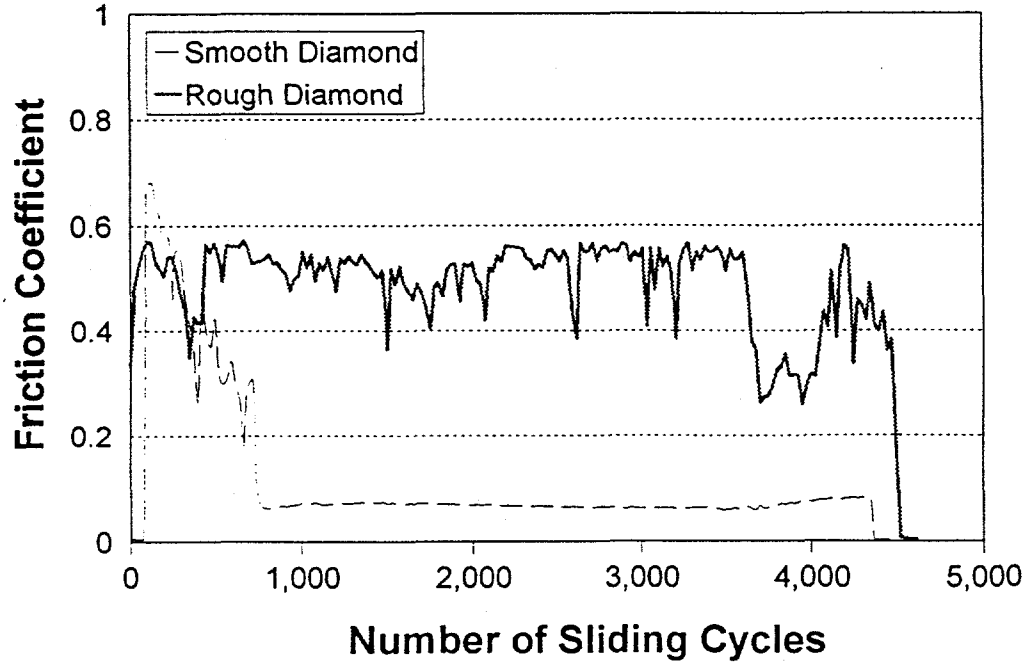

Figure 5b.

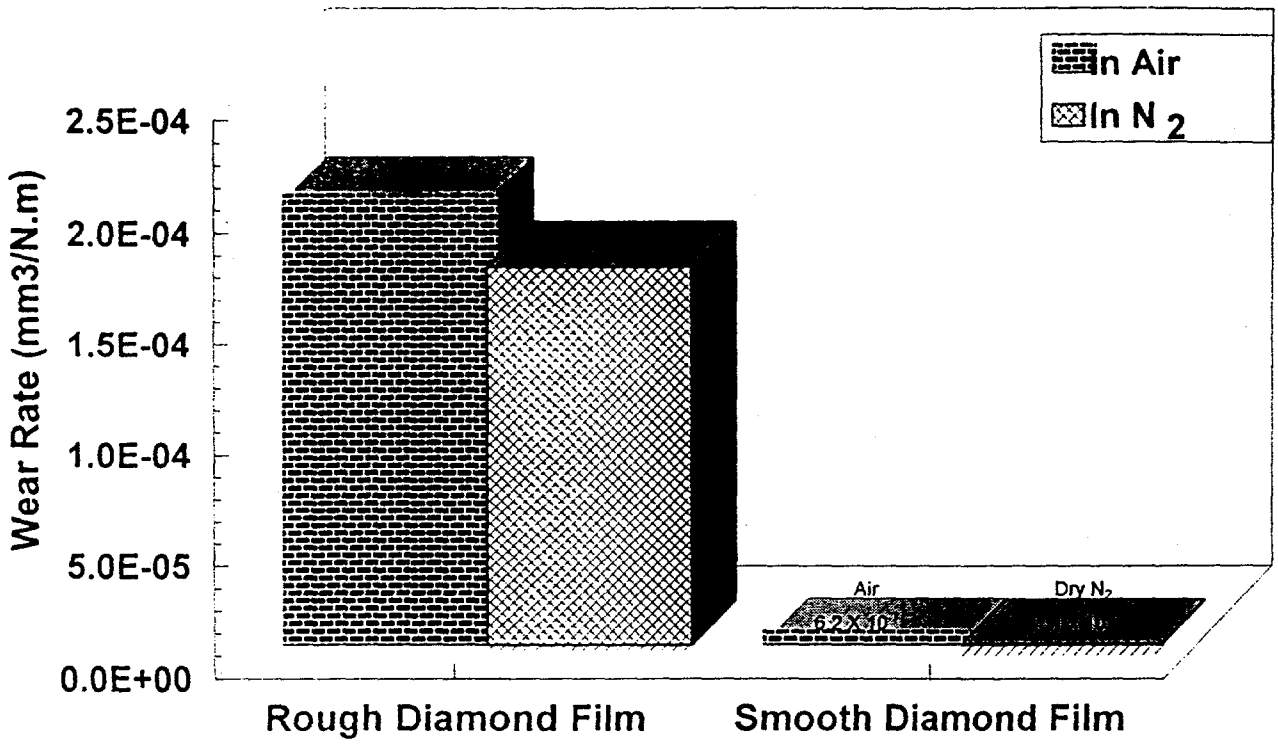
In Air
In N 2
2.5E-04
2.0E-04
1.5E-04
1.0E-04
5.0E-05
0.0E+00
Wear Rate (mm3/N.m)
Air
Dry N2
6.2X 10
Rough Diamond Film
Smooth Diamond Film

Figure 6.

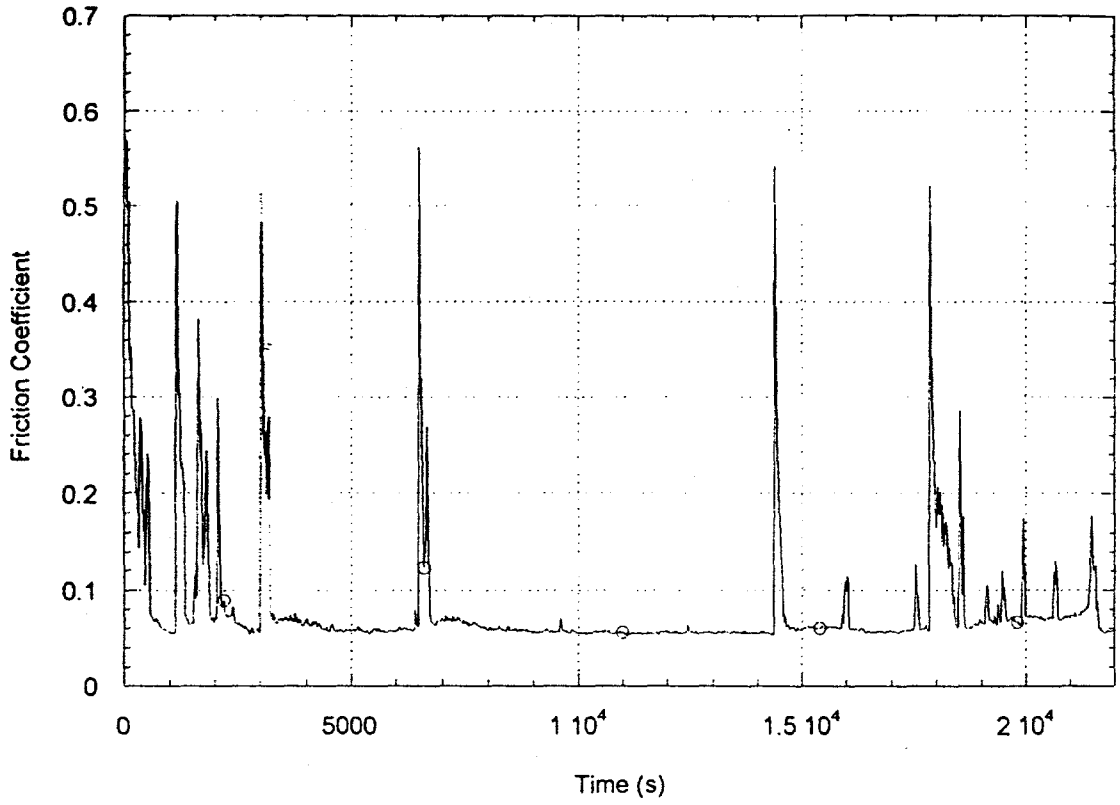
0.7
0.6
0.5
0.4
0.3
0.2
0.1
0
Friction Coefficient
0
5000
1 10^4
1.5 10^4
2 10^4
Time (s)

Figure 7.

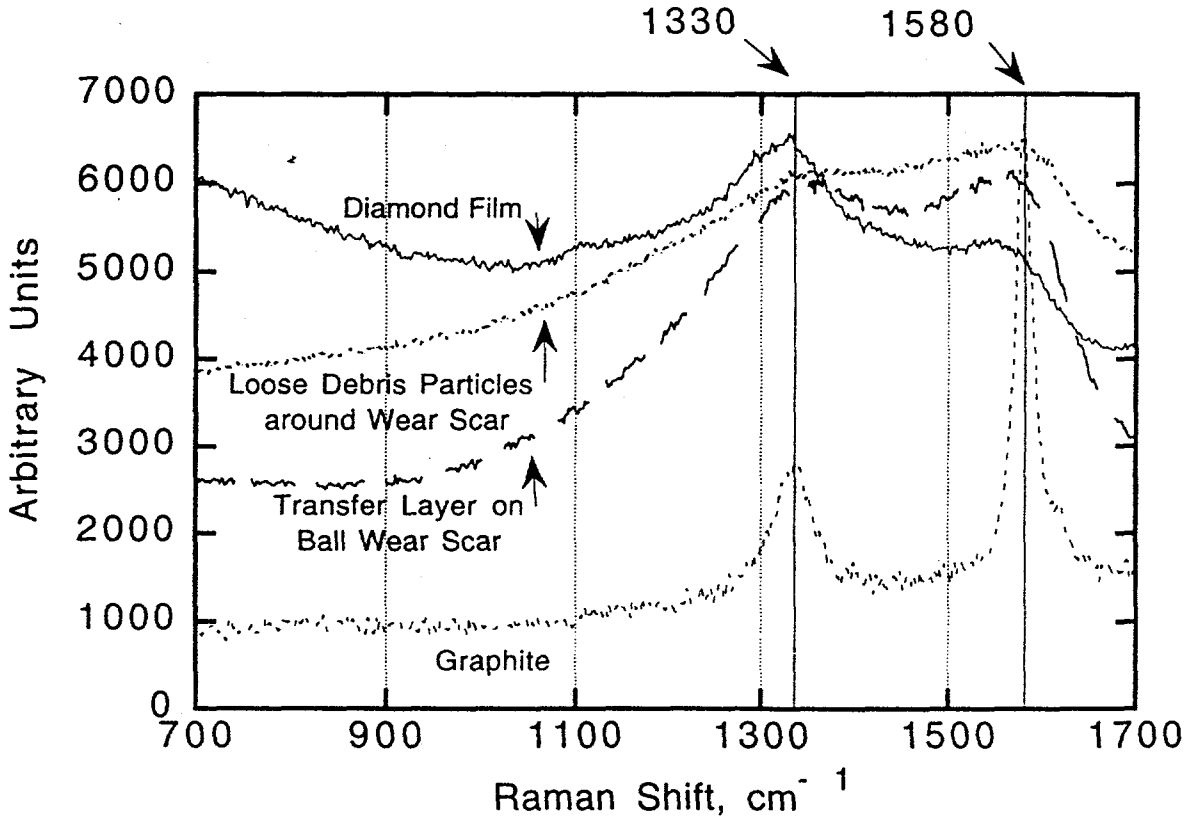
1330
1580
7000
6000
5000
4000
3000
2000
1000
0
Arbitrary Units
Diamond Film
Loose Debris Particles
around Wear Scar
Transfer Layer on
Ball Wear Scar
Graphite
700
900
1100
1300
1500
1700
Raman Shift, cm-1

Figure 8.

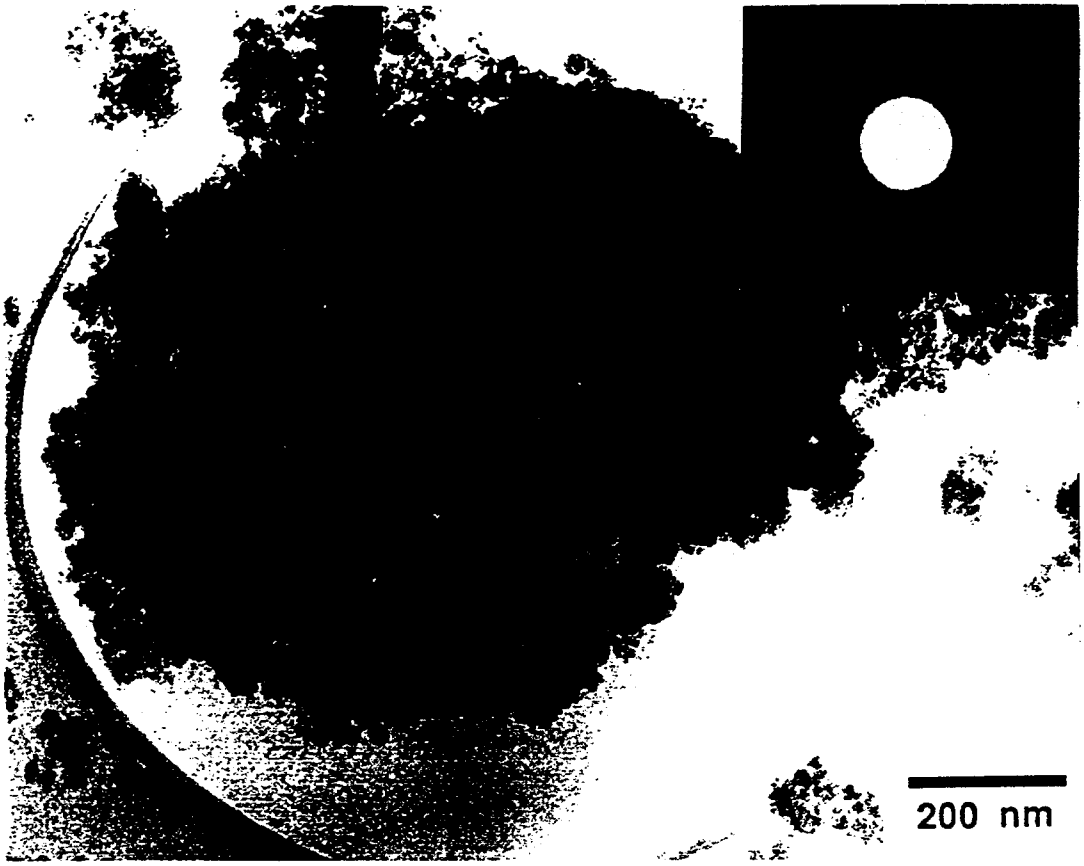

Figure 9 a.

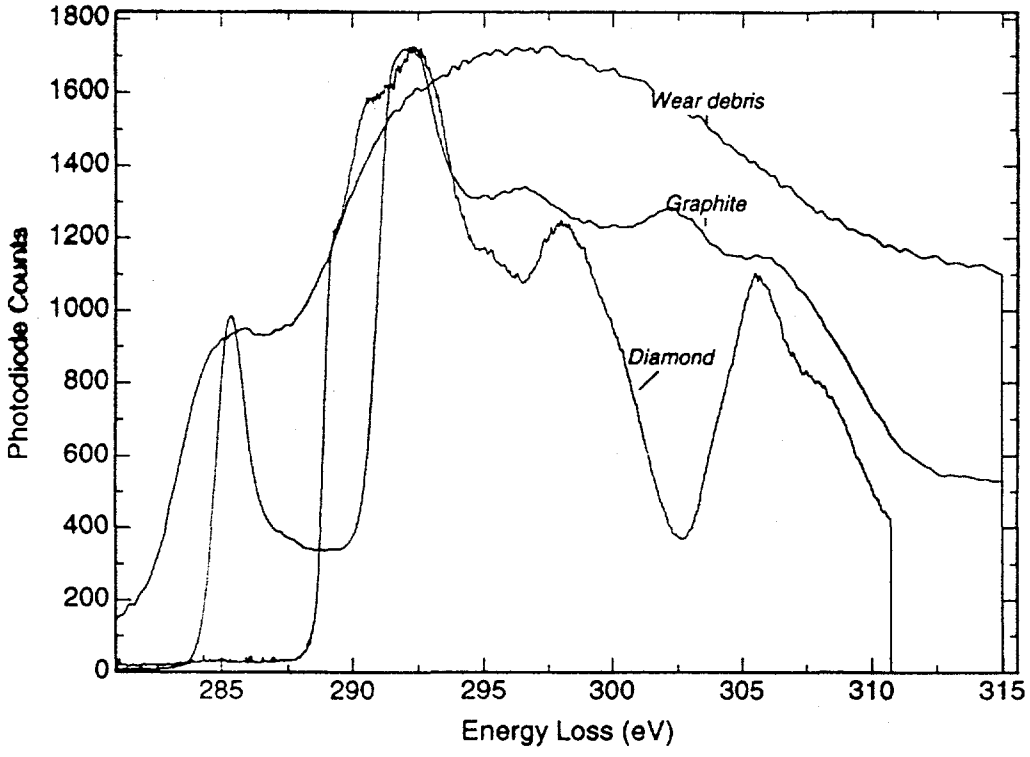

Figure 9 b.